Proceedings of the 12th International Conference on
Aluminium Alloys, September 5-9, 2010, Yokohama, Japan

pp. 2275-2280

Image-based simulation of monotonic crack propagation through a 2024 aluminum alloy

H. Tsuruta[1], H. Toda[1], P. Qu [1], M. Kobayashi[1], E. Maire[2]
[1]Department of Production System Engineering, Toyohashi University of Technology, Japan
[2]GEMPPM UMR, CNRS, France

Recently, the evaluations of the local crack driving forces have been performed by using the microstructure tracking method and direct measurement of the local crack-tip opening displacement (CTOD) respectively, which have been associated internal texture with fracture morphology. However, these experimental results are superposed by both the microstructures and crack configuration. Therefore, those influences have not been assessed separately yet. A combined methodology of the in-situ 3-D observation via synchrotron X-ray CT and the image-based numerical simulation method, which allowed for the separation of the effects of crack morphology and microstructure effects, has been performed. We have evaluated the influences of the complicated crack morphology and supposed the effects of the microstructures on the local fracture behaviors in the real material. It was identified that there is a tendency of the plasticity mixicity parameter to become locally strong along with crack deflection and tilting, and also mismatch between the crack shape and the stress field occurs due to influence with neighboring crack morphology. It was verified the characteristic region where the crack driving force would be increase approximately 1.8 times because of shielding effects from comparisons between experimental and simulation results.

Keywords: *X-ray CT; Image-based numerical simulation; Mixed-mode parameter; microstructure; local Crack driving force*

1. Introduction

Recently, the high-resolution synchrotron X-ray CT has been applied to the study of the fracture behaviors in opaque materials, which has the unique potential to provide the internal information. Actually, the crack propagates irregularly with deflecting and tilting influenced by microstructures such as pores, voids and particles, and also amount of crack growth is locally different wherever internal real material was observed[1]. The evaluations of the local crack driving forces have been performed by using the microstructure tracking method and direct measurement of the local crack-tip opening displacement (CTOD) respectively[2-4]. However, these experimental results are superposed by both the microstructures and crack configuration. Therefore, those influences have not been assessed separately yet. For instance, when a particle exists in front of the crack-tip, the crack will be slowed down or deflected such as the crack detours particle is caused by shielding effects acts to obstruct the direction of crack growth. On the other hand, when a micro pores and voids exist in front of the crack-tip, the crack will be advanced locally as if the crack was drawn into the pores and voids, due to the anti-shielding effects. It has been identified that the stress field is different from mode I load style such as the load style becomes locally mode-mixity in the vicinity of crack-tip where the crack deflection and tilting occurs. In the present work, a combined methodology of the in-situ 3-D observation via synchrotron X-ray CT and the image-based numerical simulation method has been performed. The microstructures except aluminum matrix were not considered in the model. It aimed to analyze the influences of the complicated crack morphology and the microstructures on the local fracture behaviors.

2. Experimental Methods

2.1 Tomographic experiments

In-situ observation during fracture toughness test was performed by using a white x-ray beam with photon energy of 60 keV at beam-line ID-15A of ESRF radiation facility[5]. Selected material used in this work was an Al-Cu-Mg alloy which is heat treated on the condition T361. The identical material has been studied experimentally by the present authors, and the present study has been organized for comparison purpose. An isotropic voxels with a 1.59 μm^3 edge was achieved in the reconstructed slice. Load-Displacement curve, which is obtained from in-situ observation of fracture toughness test, is shown in Fig. 1. The 3D renderings of the cracks in different load steps are shown in Fig. 2. 3D images of the crack, voids, pores, particles and aluminum matrix which was taken at loading step A and B are shown in (a) and (c). (b) and (d) were the 3D image of the region interested in the present work, which were segmented aluminum from (a) and (c) on the position 410 to 450 μm on the axis along the thickness direction. Complexity of crack morphology, local difference of crack length and diapering in-homogeneously of microstructure is identified.

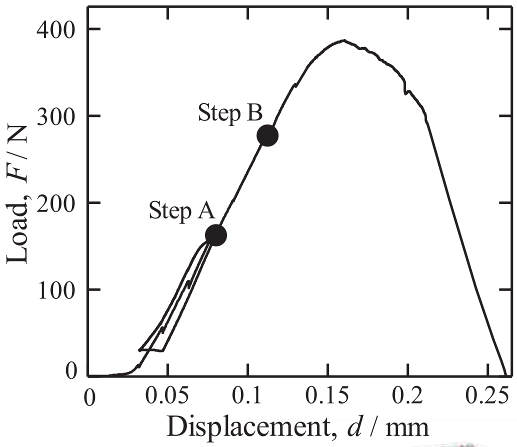

Fig. 1 Load-displacement curve in an in-situ tensile test. The crack image in load step A was used for creating the image-based model. The crack image in load step B was used for analyzing image-based model.

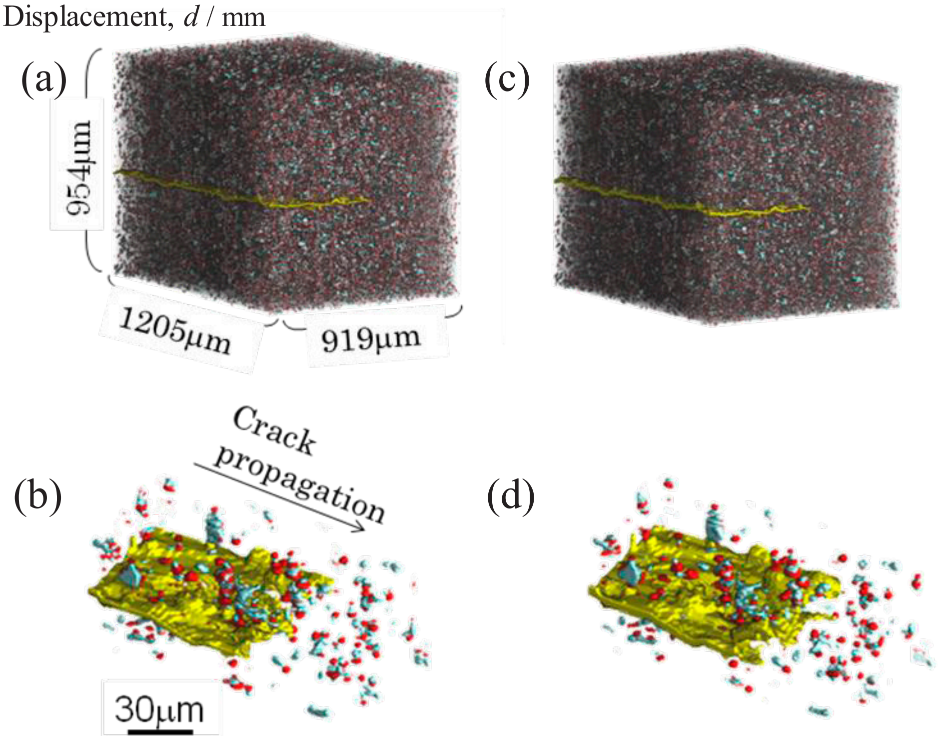

Fig. 2(a) and (c) are the three-dimensional rendering image of the crack, voids, particle and aluminum matrix at loading step A and B respectively. (b) and (d) are the 3D image of the crack with micro-pores and particles in the region, which were segmented from (a) and (c). Crack is yellow, pores and voids are red and particles are blue.

2.2 Image-based numerical simulation methodology

The 3D crack morphology at loading step A which is utilized in order to create image-based model is shown Fig. 3(a). In order to reduce calculation cost, the surface mesh model of the crack is consisted of fine mesh in the region of interest and coarse mesh in the other regions is shown in Fig. 3(b). In the next place, the outer edge of the material was created, then 3D image-based simulation model was constructed that divided between the surface mesh model of the crack and outer edge of the material using tetrahedral elements[6,7]. Complex morphology, such as the crack deflection and tilting, has been modeled with a high accuracy in the analysis region and all of the microstructures were eliminated in the model. Then elastic- plastic FEM analysis which is monotonic tensile test has been carried out that forced displacement of loading step B is applied.

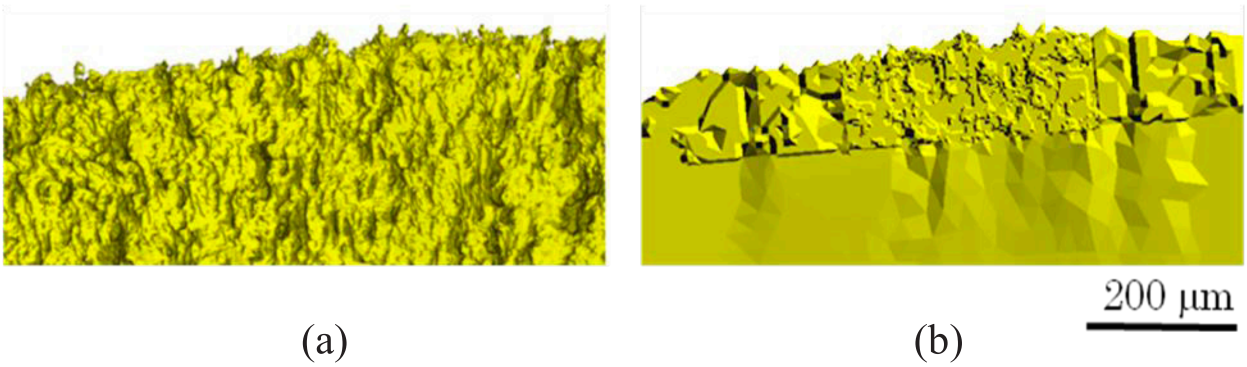

Fig. 3 (a)Top view of the three-dimensional crack image at loading step A, which was utilized to create the image-based model. (b)Top view of the surface mesh of the model, which was consisted of fine mesh and coarse mesh part.

3. Simulation Results

3.1 Relationship between crack shape and mixed-mode parameter

In order to figure out the influence of the crack morphology on the stress field in the vicinity of crack tip, the plasticity mixicity parameter was calculated along the crack front line shown in Fig. 2(d), where the crack deflection and tilting were observed. Eq. 1 and Eq. 2 was used to calculate the plasticity mixicity parameter along the crack front line. When the plasticity mixicity parameter converges to 0, it means only mode Ⅰ loading acted on the crack-tip.

$$Mp^{I\text{-}II} = \left| \lim_{r \to 2\delta} \frac{\sigma_{r\theta}(r, \theta = 0)}{\sigma_{\theta\theta}(r, \theta = 0)} \right| \times 100 \quad (\%) \tag{1}$$

$$Mp^{I\text{-}III} = \left| \lim_{r \to 2\delta} \frac{\sigma_{\theta z}(r, \theta = 0)}{\sigma_{\theta\theta}(r, \theta = 0)} \right| \times 100 \quad (\%) \tag{2}$$

The calculation results are shown in Fig. 4. Vertical axis indicates the plasticity mixicity parameter together with deflection angle measured on the crack image in load step B. It was identified that $Mp^{I\text{-}II}$ and $Mp^{I\text{-}III}$ increased in connection with the crack deflection and tilting, the stress field would be locally mixed-mode loading style near the crack-tip.

3.2 Relationship between crack morphology and plastic zone size

The shape and size of the plastic zone a head of crack-tip, should vary with the loading mode. Plastic zone shape will be kidney bean shaped when subjected to a pure mode Ⅰ loads[8,9]. The calculated results of aforementioned mixed-mode parameter and plastic zone size is plotted in Fig. 5. We found that the plastic zone size increased with the increase of the mixed-mode parameter in general. As we know, the pure mode II and mode III cracks have much larger plastic zones than the pure mode I crack with the same load level. Therefore, the aforementioned relationship between the plastic zone size and the mixed-mode parameter indicates that the near-tip strain fields were changed due to the local mixed-mode loading on crack tip.

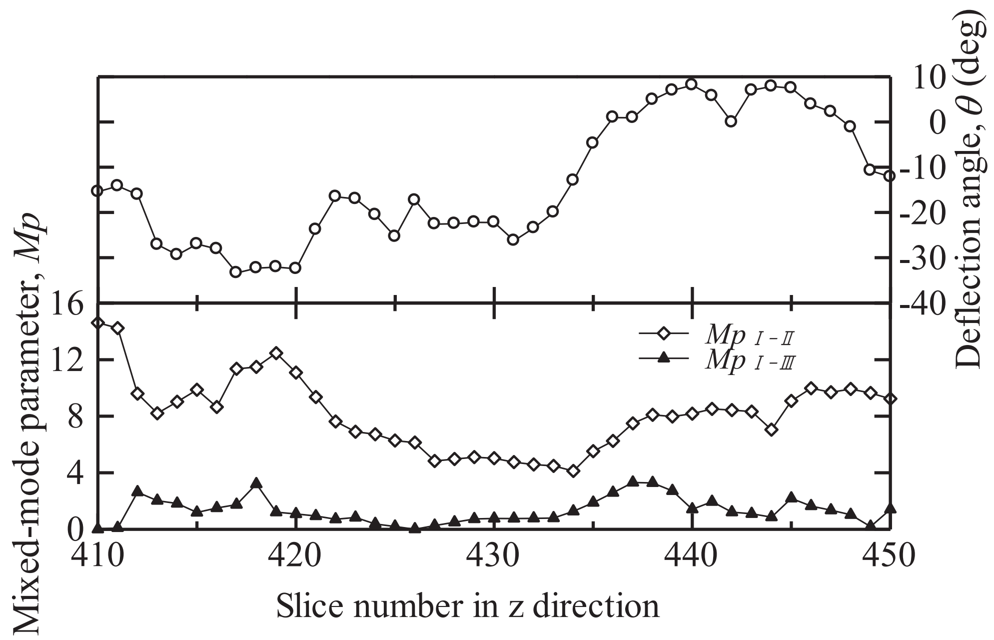

Fig. 4 Variations of mode-mixity parameter in mode Ⅰ－Ⅱ and Ⅰ-Ⅲ along crack front line obtained from the image-based models.

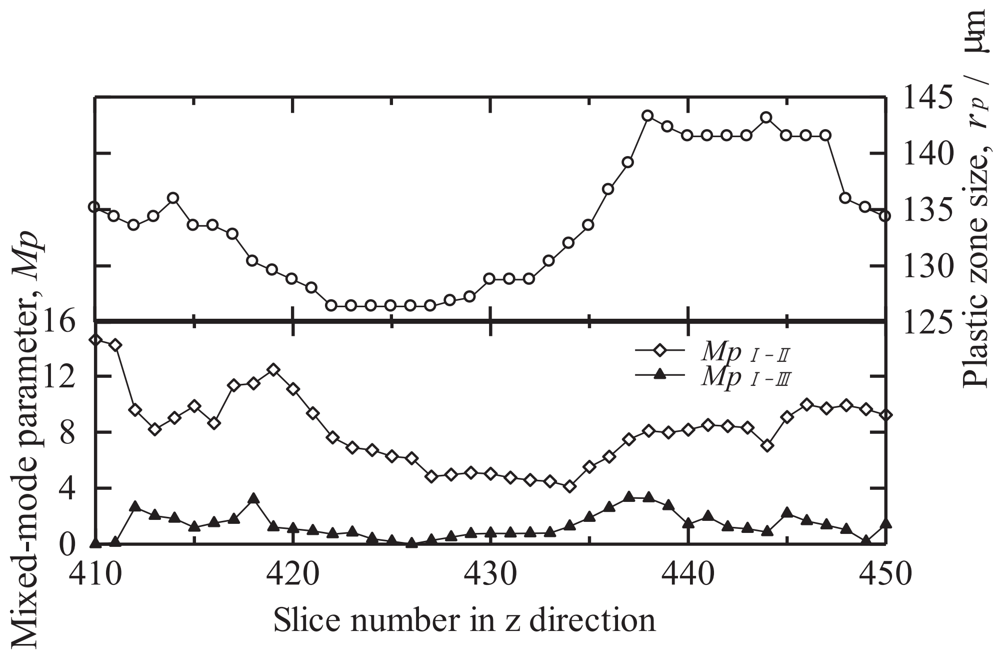

Fig. 5 Variation of the plastic zone size distributions along the crack front line (simulation results).

3.3 The stress field would be changed along with neighboring crack

Fig. 6(a) shows the contour map of the equivalent plastic strain on a slice containing a crack with a deflection on crack tip. It was found that the plastic zone size was expanded in the load direction by the crack deflection. Fig. 6(b) shows the contour map of the equivalent plastic strain on the slice which is 10μm away from slice (a) along the thickness direction. Although the crack morphology was almost straight, the plastic zone shape was asymmetric with respect to the global crack advanced plane. It is indicated that the mismatch occurs between the crack shape and the stress field because of the (b) section being influenced by neighboring crack morphologies which is due to the influence of the deflected crack in slice (a).

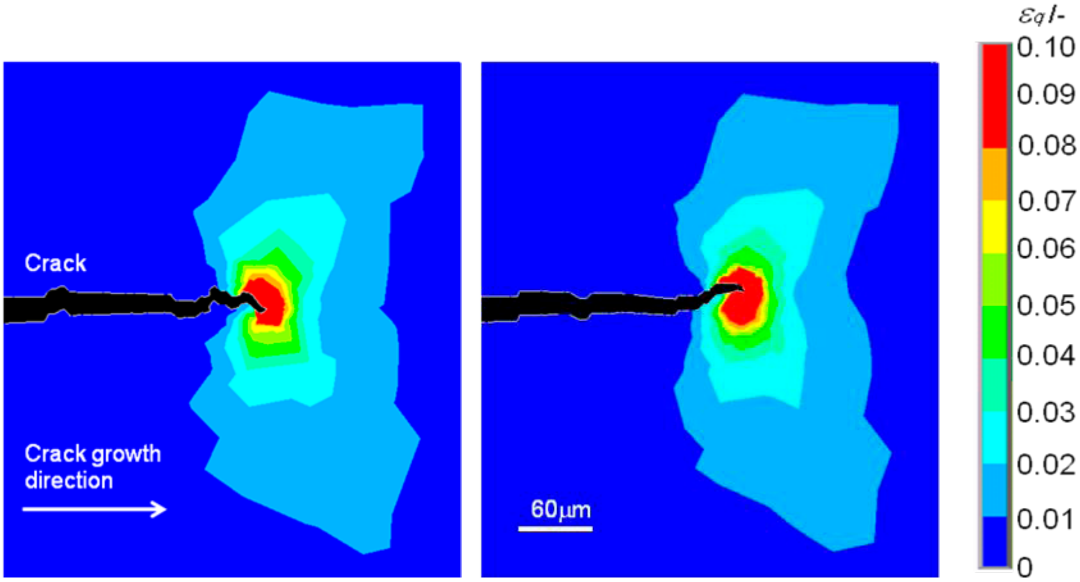

(a)Slice470 (b)Slice463

Fig.6 Contour maps of the equivalent plastic strain on two neighboring slices.

3.4 The comparison of experiment with simulation through local crack driving force

The experimental results and the simulation results of J-integral measured on every slice along the thickness direction are plotted in Fig. 7. The experimental results were affected by the microstructures of the specimen compared with the simulation results. It is found that the simulation results are approximately 1.8 times higher than experimental result from slice numbers 410 to 415, because many pores and voids existed in the vicinity of the crack tip which is those microstructure contributed in decreasing the local crack driving force. Similar discrepancy is seen between 438 and 443, resulting from the identical reason. On the other hand, the experimental results are approximately 1.5 times higher than the simulation results between the slice numbers 425 to 430. This discrepancy was due to a few particles existing in the vicinity of crack tip, which contributed to increase the local crack driving force. Influence of the crack shape was separated as a result of comparison of experimental results with simulated results, it has been presumed influence on local fracture behaviors by the effect of the microstructures.

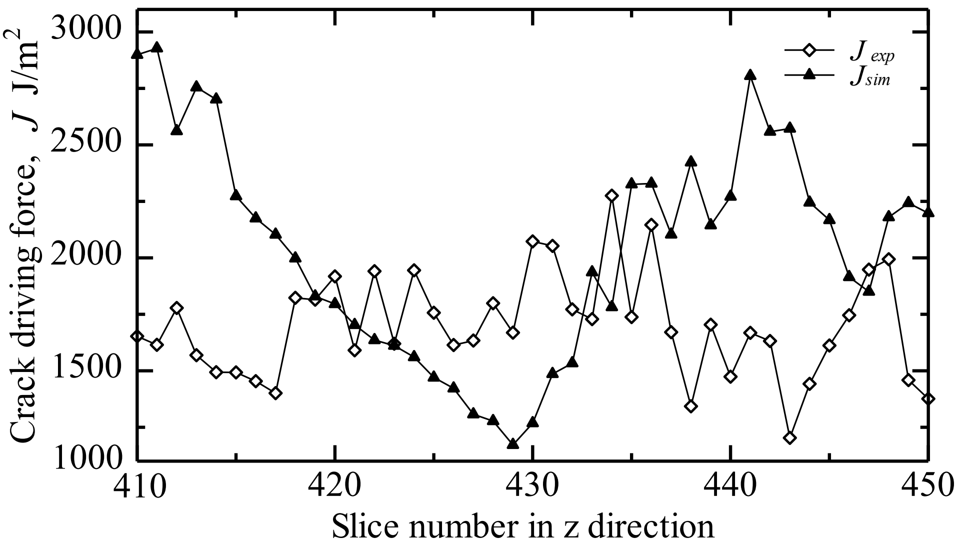

Fig. 7 Variation of J-integral along the crack front line.

4. Conclusion

Image-based numerical simulation has been carried out using the high-resolution micro tomography images in order to separate the effects of crack morphology from those of microstructure, such as micro-pores, voids and particles. We have evaluated how local complex crack-tip morphology and microstructure influences tensile fracture behaviors in real material. It has been clarified that mode-mixicity increases as mode II / III loading state is enhanced the region with a deflected and /or tilted. It has been inferred by comparing with experiments that local crack driving forces are enhanced due to the existence of pores in the vicinity of a crack-tip, thereby promoting complex crack–microstructure interactions.

Acknowledgment

The synchrotron radiation experiments were performed with the approval of helping in the ESRF. I would like to thank sincerely Prof. Toda, Mr. Qu, Mr. Kobayashi and Mr. Maire for instructing and supporting.

References

[1] H. Zhang, H. Toda, P.C. Qu, Y. Sakaguchi, M. Kobayashi, K. Uesugi, Y. Suzuki, Acta Materialia 57 (2009) 3287–3300

[2] P. Qu, H. Toda, H. Zhang, Y. Sakaguchi, L. Qian, M. Kobayashi, K. Uesugi, Scripta Materialia 61 (2009) 489–492

[3] A. Miyawaki, Master's thesis, Toyohashi University of Technology, Toyohashi, 2008.

[4] H. Toda, S. Yamamoto, M. Kobayashi, K. Uesugi, H.Zhang, Acta Mater. 56 (2008) 6027.

[5] T. Hiramatsu, Master's thesis, Toyohashi University of Technology, Toyohashi, 2009.

[6] L. Qian, H. Toda, K. Uesugi, M. Kobayashi, and T. Kobayashi, PHISICAL LETTERS (21 March 2008) 115505-1-4

[7] A. Gonz_alez-Herrera, J. Zapatero, Engineering Fracture Mechanics 72 (2005) 337–355

[8]Fracture Mechanics 2nd edition p. 38-42

[9]Fracture Mechanics 2nd edition p. 79-82